Journal of Materials Chemistry A

RSC Publishing

PAPER

Unique core–shell structured $SiO_2(Li^+)$ nanoparticles for high-performance composite polymer electrolytes

Cite this: *J. Mater. Chem. A*, 2013, **1**, 395

Seo Hee Ju,[a] Yoon-Sung Lee,[a] Yang-Kook Sun[b] and Dong-Won Kim*[a]

Received 28th August 2012
Accepted 7th October 2012

DOI: 10.1039/c2ta00556e

www.rsc.org/MaterialsA

Core–shell structured SiO_2 nanoparticles with controlled morphology were synthesized and used as functional fillers in Li^+-conducting composite polymer electrolytes for lithium-ion polymer batteries. The composite polymer electrolytes prepared with poly(vinylidene fluoride-*co*-hexafluoropropylene) and core–shell $SiO_2(Li^+)$ nanoparticles exhibited high ionic conductivity, good mechanical strength and favorable interfacial characteristics. Tests run on carbon/$LiNi_{1/3}Co_{1/3}Mn_{1/3}O_2$ cells with composite polymer electrolyte containing optimized $SiO_2(Li^+)$ nanoparticles yielded excellent results in terms of capacity retention (95% after 100 cycles) and rate capability (167 mA h g^{-1} at 5 C rate).

Introduction

Solid polymer electrolytes such as poly(ethylene oxide) (PEO) have received much attention in rechargeable lithium batteries due to enhanced safety, absence of leakage of organic solvents and design flexibility.[1–5] However, these materials have a major drawback that the ionic conductivity for practical application can only be reached at high temperatures. To overcome this problem, most relevant research has focused on the preparation and characterization of gel polymer electrolytes that exhibit high ionic conductivities at room temperature.[5–8] Though these gel polymer electrolytes show high ionic conductivities comparable to those of liquid electrolytes, incorporation of a large amount of liquid electrolyte is detrimental to their mechanical properties. Thus, a microporous polyolefin separator is now being used as a mechanical support in commercialized lithium-ion polymer batteries. It has been reported that the addition of ceramic fillers such as SiO_2, Al_2O_3, TiO_2 and $BaTiO_3$ into polymer electrolytes improved the electrical and mechanical properties.[9–17] In these composite polymer electrolytes, the ceramic particles promote electrochemical properties of the polymer electrolytes, but only by physical action without directly contributing to the lithium ion transport process. These ceramic particles can also act as a source of charge carriers by facilitating suitable surface modifications of particles.[18–20] In our previous studies, the core–shell structured SiO_2 particles containing lithium ions in their shell were synthesized and used as functional fillers in Li^+-conducting composite polymer electrolytes.[21,22] These fillers have a very uniform spherical shape, and the SiO_2 core is covalently bonded to poly(lithium 4-styrenesulfonate) (PLSS) in the shell layer. However, the size of the core–shell SiO_2 particles was very large (~2.0 μm) and their morphologies as functional fillers were not optimized with respect to core diameter and shell thickness.[21] It was thought that the core diameter should be more reduced to the nanometer scale and the shell thickness should be optimized to give the improved transport and interfacial properties as fillers in composite polymer electrolytes for lithium-ion polymer batteries.

Hence, in this work presented here, we report the properties and electrochemical characteristics of composite polymer electrolytes based on core–shell structured SiO_2 nanoparticles with controlled morphology with respect to core diameter and shell thickness. A detailed investigation on the effect of shell thickness has been made to provide the composite polymer electrolytes with high ionic conductivity, good mechanical strength and favorable interfacial characteristics. The composite polymer electrolytes are applied to the lithium-ion polymer batteries composed of a graphite anode and a $LiNi_{1/3}Co_{1/3}Mn_{1/3}O_2$ cathode. We demonstrate that the composite polymer electrolytes containing core–shell SiO_2 nanoparticles with optimized core diameter and shell thickness are very promising electrolyte materials for high performance lithium-ion polymer batteries.

Experimental

Synthesis of $SiO_2(Li^+)$ nanoparticles

Fig. 1 illustrates the synthetic scheme of core–shell structured $SiO_2(Li^+)$ particles. Vinyltrimethoxylsilane (VTMS, 2 ml) was added to 150 ml of double distilled water with stirring until the VTMS droplets completely disappeared. 10 ml of ammonium hydroxide solution (28 wt%) was then added to the solution and the reaction was continued for 12 h at room temperature. After completion of the reaction, the resulting precipitate was

[a]*Department of Chemical Engineering, Hanyang University, Seungdong-Gu, Seoul 133-791, Republic of Korea. E-mail: dongwonkim@hanyang.ac.kr; Fax: +82 2 2220 4337; Tel: +82 2 2220 2337*

[b]*Department of WCU Energy Engineering, Hanyang University, Seungdong-Gu, Seoul 133-791, Republic of Korea*

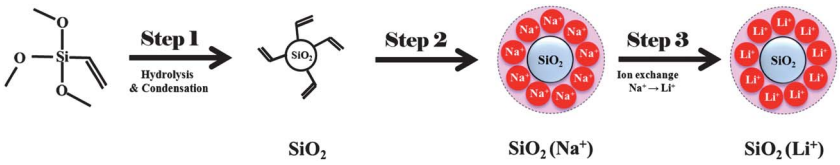

Fig. 1 Reaction scheme for synthesis of the SiO_2 core with vinyl groups, core–shell structured $SiO_2(Na^+)$ and $SiO_2(Li^+)$ particles.

centrifuged and washed several times with ethanol. The core–shell $SiO_2(Na^+)$ particles were synthesized by radical copolymerization of cored-silica particles (1.5 g) and 4-styrenesulfonic acid sodium salt (4.0–6.0 g) with azobisisobutyronitrile (0.4 g) in 140 ml of *n*-methyl pyrrolidone (NMP) at 60 °C. The shell thickness could be controlled by varying the concentration of the 4-styrenesulfonic acid sodium salt monomer and the reaction time from 24 to 72 h. After polymerization, the solution was precipitated in a large excess of diethyl ether. The precipitate was filtered and washed several times with methanol/ethanol. The Na^+ ions in the core–shell structured SiO_2 particles were replaced by Li^+ ions by ionic exchange with $LiOH \cdot H_2O$.

Preparation of composite polymer electrolytes

A composite polymer membrane consisting of poly(vinylidene fluoride-*co*-hexafluoropropylene) (P(VdF-*co*-HFP)) and core–shell structured $SiO_2(Li^+)$ nanoparticles was prepared by mixing P(VdF-*co*-HFP), $SiO_2(Li^+)$ powders and dibutyl phthalate (DBP) (40 : 10 : 50 by weight) in acetone by ball milling, and casting using a doctor blade. The membrane was immersed in methanol to remove DBP and then vacuum dried at 70 °C for 12 h. The core–shell $SiO_2(Li^+)$ content in the composite polymer membranes was fixed at 20 wt% based on the dry polymer membrane containing polymer and core–shell $SiO_2(Li^+)$ particles, according to our previous work.[21] Free-standing composite polymer electrolyte films were finally obtained by soaking the membrane in 1.15 M $LiPF_6$–ethylene carbonate (EC)/diethyl carbonate (DEC) (3 : 7 by volume, battery grade, Soulbrain Co.). The uptake of the liquid electrolyte solution was determined by the equation:

$$\text{Uptake } (\%) = (W_g - W_m)/W_m \times 100 \quad (1)$$

where W_g and W_m are the weights of the polymer electrolyte and dry membrane, respectively.

Electrode preparation and cell assembly

The $LiNi_{1/3}Co_{1/3}Mn_{1/3}O_2$ electrode was prepared by coating a NMP-based slurry containing $LiNi_{1/3}Co_{1/3}Mn_{1/3}O_2$ (3 M), poly(vinylidene fluoride) (PVdF) and super-P carbon (MMM Co.) (85 : 7.5 : 7.5 by weight) onto an Al foil. A carbon electrode was similarly prepared by coating an NMP-based slurry of mesocarbon microbeads (MCMB, Osaka gas), PVdF and super-P carbon (88 : 8 : 4 by weight) onto a copper foil. Lithium-ion polymer cells were assembled by sandwiching the composite polymer electrolyte between the carbon anode and the $LiNi_{1/3}Co_{1/3}Mn_{1/3}O_2$ cathode. For comparison, a liquid electrolyte-based lithium-ion cell was also assembled with a polypropylene separator (Celgard 2400) and the same liquid electrolyte (1.15 M $LiPF_6$–EC/DEC) instead of a composite polymer electrolyte. The cells were enclosed in a metallized plastic bag and vacuum-sealed.

Characterization and electrochemical evaluation

The morphologies of the materials were examined using a scanning electron microscope (SEM, JEOL JSM-6300) and a transmission electron microscope (TEM, Tecnai G2 F30). The presence of lithium ions in core–shell structured SiO_2 particles was confirmed by Auger electron spectroscopy (AES, ULVAC-PHI, PHI 700). The lithium transport number was measured by a combination of AC impedance and DC polarization methods.[23] AC impedance measurements were performed to measure ionic conductivity and interfacial resistance using an impedance analyzer over a frequency range of 1 mHz to 100 kHz with an amplitude of 10 mV. Charge and discharge cycling tests of the lithium-ion polymer batteries were conducted over a voltage range of 3.0–4.5 V with battery test equipment at room temperature.

Results and discussion

Spherical silica core particles with an average particle size ranging from 200 to 1210 nm were synthesized, as shown in Fig. 2. From the FT-IR spectra of these silica core particles, we found peaks corresponding to siloxane (Si–O–Si) groups (766, 1000–1200 cm^{-1}) and the C=C double bonds (1410, 1603 cm^{-1}). These results imply that the silica core particles contain reactive vinyl groups for permitting the growth of silica core particles by radical polymerization with 4-styrenesulfonic acid sodium salt. The silica core particles with small particle size proved to be effective as fillers for composite polymer electrolytes in our study, and thus particles with an average diameter of 200 nm were chosen as the base material for synthesizing core–shell structured SiO_2 particles. Silica core particles with an average diameter less than 200 nm could not be obtained. Core–shell structured SiO_2 particles were obtained by radical copolymerization of silica core particles and the sodium 4-styrenesulfonate monomer. Fig. 3 shows the TEM images of core–shell silica particles containing poly(sodium 4-styrenesulfonate) (PSSS) in the shell. All particles exhibit very uniform core–shell morphology with a shell layer of PSSS (in gray) surrounding a SiO_2 core particle (in black). The core diameter was about 200 nm, and the shell thickness was measured to be 120, 240 and 320 nm, respectively. Unfortunately, we could not synthesize the core–shell SiO_2 particles

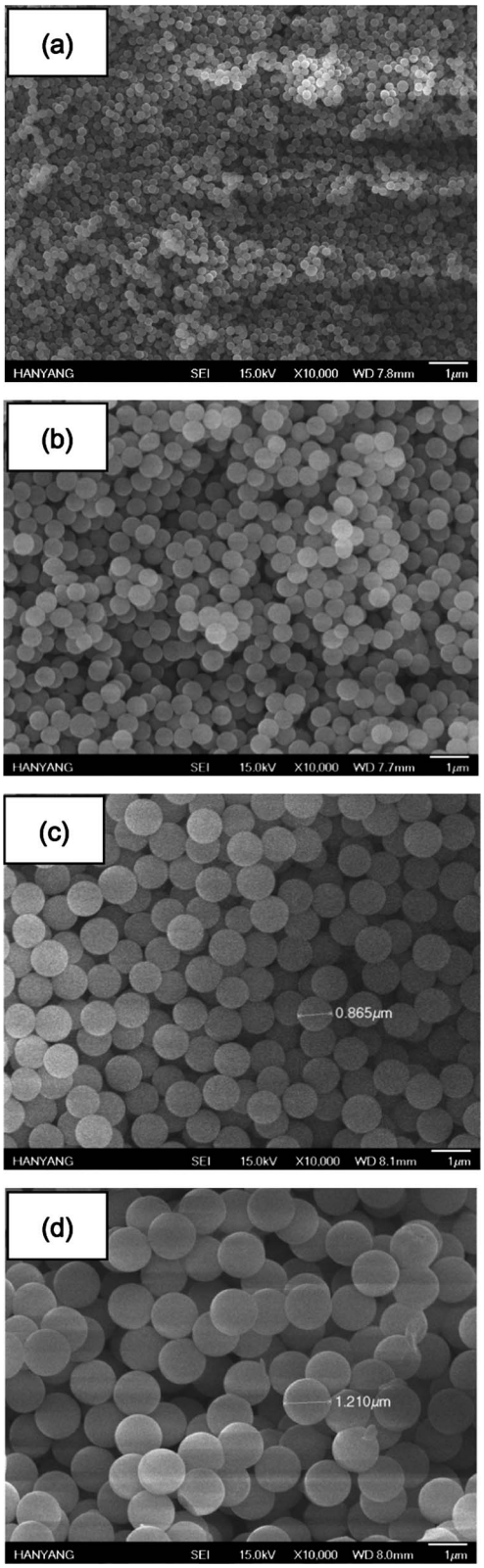

Fig. 2 SEM images of SiO_2 core particles with different particle sizes. The average particle sizes are (a) 200 nm, (b) 490 nm, (c) 865 nm and (d) 1210 nm.

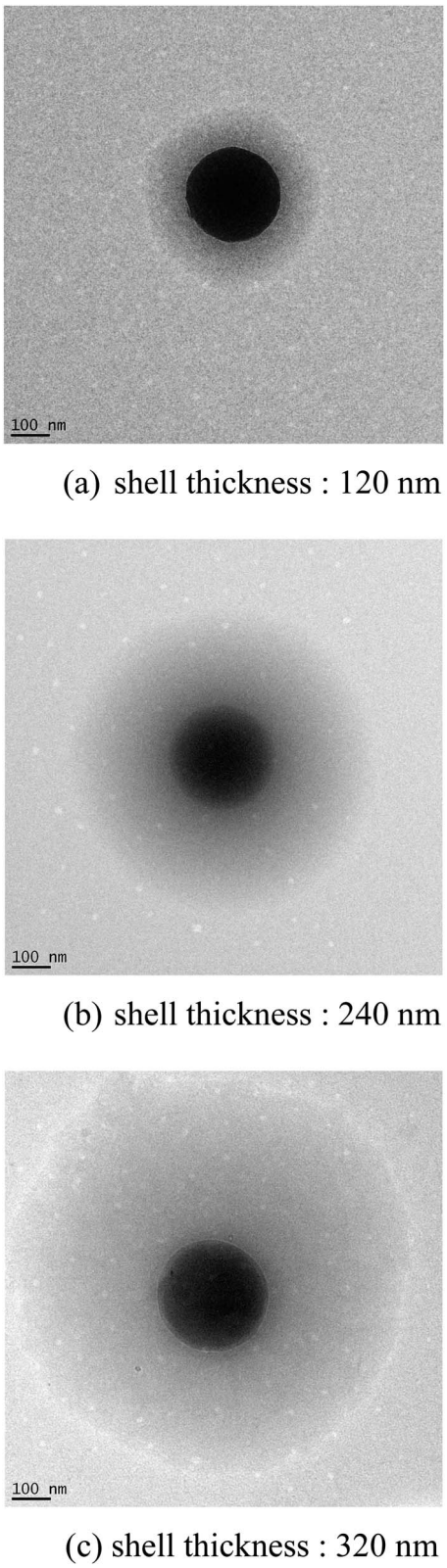

Fig. 3 TEM images of core–shell structured SiO_2 particles with different shell thicknesses of (a) 120 nm, (b) 240 nm and (c) 320 nm.

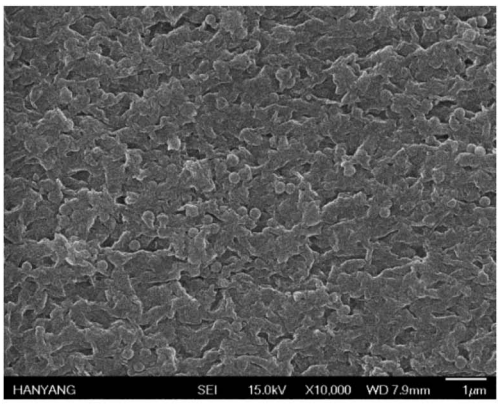

(a)

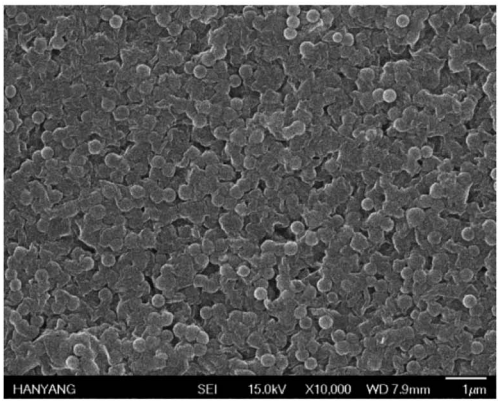

(b)

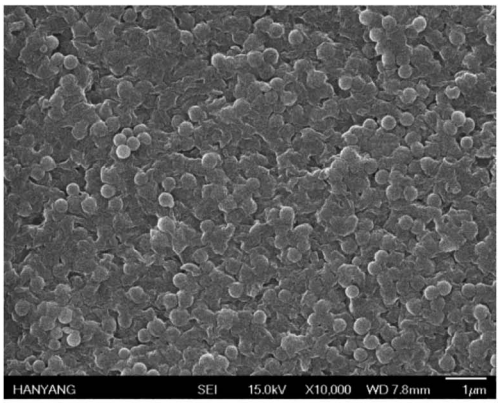

(c)

Fig. 4 SEM images of composite polymer membranes containing 20 wt% core–shell structured $SiO_2(Li^+)$ nanoparticles with a shell thickness of (a) 120 nm, (b) 240 nm and (c) 320 nm.

with uniform shell thickness larger than 320 nm, even if the concentration of the 4-styrenesulfonic acid sodium salt monomer or the reaction time was increased. Using these core–shell structured SiO_2 particles, we replaced the sodium ions in the shell layer (PSSS) of the core–shell structured SiO_2 particles with lithium ions. An Auger electron spectroscopy profile of the $SiO_2(Li^+)$ particles revealed a 54.8 eV characteristic peak corresponding to lithium,[24] confirming that the $SiO_2(Na^+)$ particles were converted to $SiO_2(Li^+)$ particles.

Composite polymer membranes were prepared from P(VdF-*co*-HFP) and core–shell $SiO_2(Li^+)$ nanoparticles. Fig. 4 shows the SEM images of the composite polymer membranes containing 20 wt% core–shell SiO_2 particles with different shell thicknesses. As shown in the figure, the membranes showed very homogeneous morphology, and no silica agglomeration could be observed on the membrane surface. The EDAX mapping images shown in Fig. 5 also illustrate the homogeneous distributions of chosen elements (fluorine, silicone, and sulfur) across the image, which suggests that the SiO_2 nanoparticles are homogeneously distributed in the composite membrane without agglomeration. The introduction of the covalent

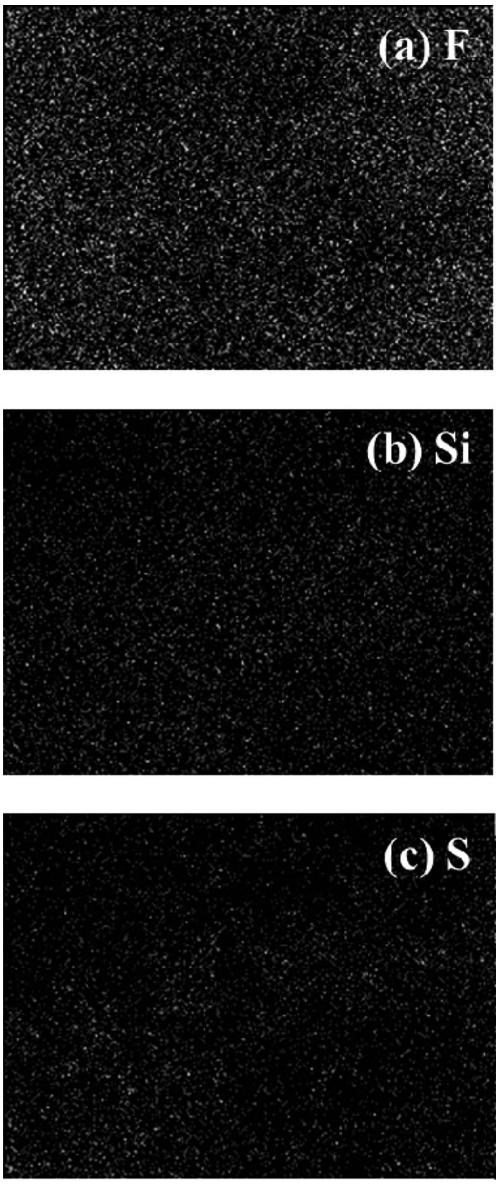

Fig. 5 EDAX mapping images of (a) fluorine, (b) silicone and (c) sulfur in the composite polymer membrane containing 20 wt% core–shell structured $SiO_2(Li^+)$ particles with a shell layer of 320 nm.

Table 1 Electrolyte uptake, ionic conductivities and lithium transport number of the composite polymer electrolytes containing core–shell $SiO_2(Li^+)$ particles with different shell thicknesses

Shell thickness (nm)	Electrolyte uptake (%)	Ionic conductivity (S cm^{-1})	Li^+ transport number
120	155	9.2×10^{-4}	0.44
240	161	1.3×10^{-3}	0.49
320	179	1.7×10^{-3}	0.53

bonding between the SiO_2 core and the PLSS shell resulted in reinforcing interfacial contact between the PLSS in the shell of the SiO_2 particles and the P(VdF-*co*-HFP) matrix. As a result, homogeneous silica dispersion could be successfully obtained in the composite polymer membrane.

Composite polymer electrolyte was obtained by soaking the composite polymer membrane in liquid electrolyte. The liquid electrolyte was well encapsulated in the composite polymer membrane by physical gelation. Electrolyte uptake and ionic conductivities of composite polymer electrolytes containing $SiO_2(Li^+)$ particles with different shell thicknesses are summarized in Table 1, demonstrating that both properties increase with increasing shell thickness of $SiO_2(Li^+)$ particles. An increase in ionic conductivity with shell thickness is associated with enhanced electrolyte uptake, as well as with an increase in mobile lithium ions dissociating out of the shell of the $SiO_2(Li^+)$ particles. The hydrophilic PLSS in the shell of core–shell $SiO_2(Li^+)$ particles has a high affinity for the electrolyte solution, and thus the uptake of electrolyte increased with increasing shell thickness, which resulted in an increase of ionic conductivity. Li^+ ions dissociated from the $SiO_2(Li^+)$ particles also contribute to the ionic conductivity. It can be seen from Table 1 that the lithium transport number increases with increasing shell thickness. The $SiO_2(Li^+)$ particles are intrinsic single ion conductors, since the sulfonate anions ($-SO_3^-$) are anchored to pendant groups on the polymer around the silica core. The number of lithium ions contributing to ionic conductivity increases with increasing shell thickness as illustrated in Fig. 6, resulting in an increase of lithium transport number with shell thickness. The addition of $SiO_2(Li^+)$ nanoparticles also resulted in a filler network providing sufficient mechanical integrity to the composite polymer electrolyte. As a result, the preparation of a free-standing film with a thickness of 30 μm was possible, thereby eliminating the need for additional mechanical supports such as polyolefin separators.

Composite polymer electrolytes were used to assemble lithium-ion polymer cells composed of a carbon anode and a $LiNi_{1/3}Co_{1/3}Mn_{1/3}O_2$ cathode. Fig. 7(a) shows typical charge and discharge curves of the lithium-ion polymer cell assembled with composite polymer electrolyte containing $SiO_2(Li^+)$ particles with a shell thickness of 320 nm. The cell delivers a high initial discharge capacity of 179.0 mA h g^{-1} based on the $LiNi_{1/3}Co_{1/3}Mn_{1/3}O_2$ active material, indicating very low internal cell resistance. The cell exhibits stable cycling characteristics, that is, the cell delivers 95% of the initial discharge capacity after 100 cycles. Fig. 7(b) shows the discharge capacity *versus* cycle number of lithium-ion polymer cells assembled with composite polymer electrolyte containing different $SiO_2(Li^+)$ particles. For the purpose of comparison, the cycling result of the cell assembled with liquid electrolyte is also given in the figure. It should be noted that the cells assembled with composite polymer electrolytes containing $SiO_2(Li^+)$ particles

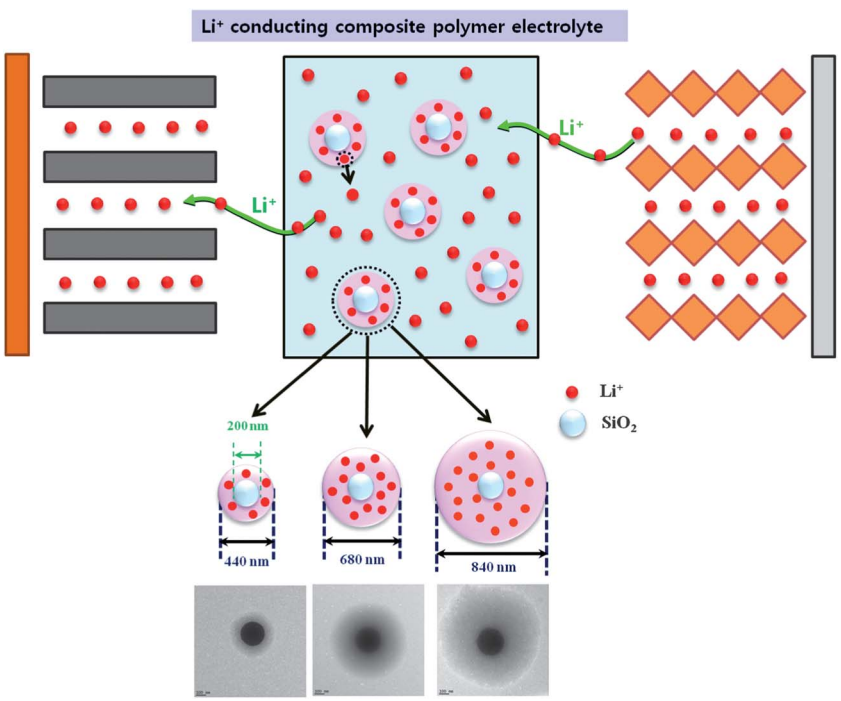

Fig. 6 Composite polymer electrolyte containing core–shell structured $SiO_2(Li^+)$ nanoparticles with different shell thicknesses for the lithium-ion polymer cell.

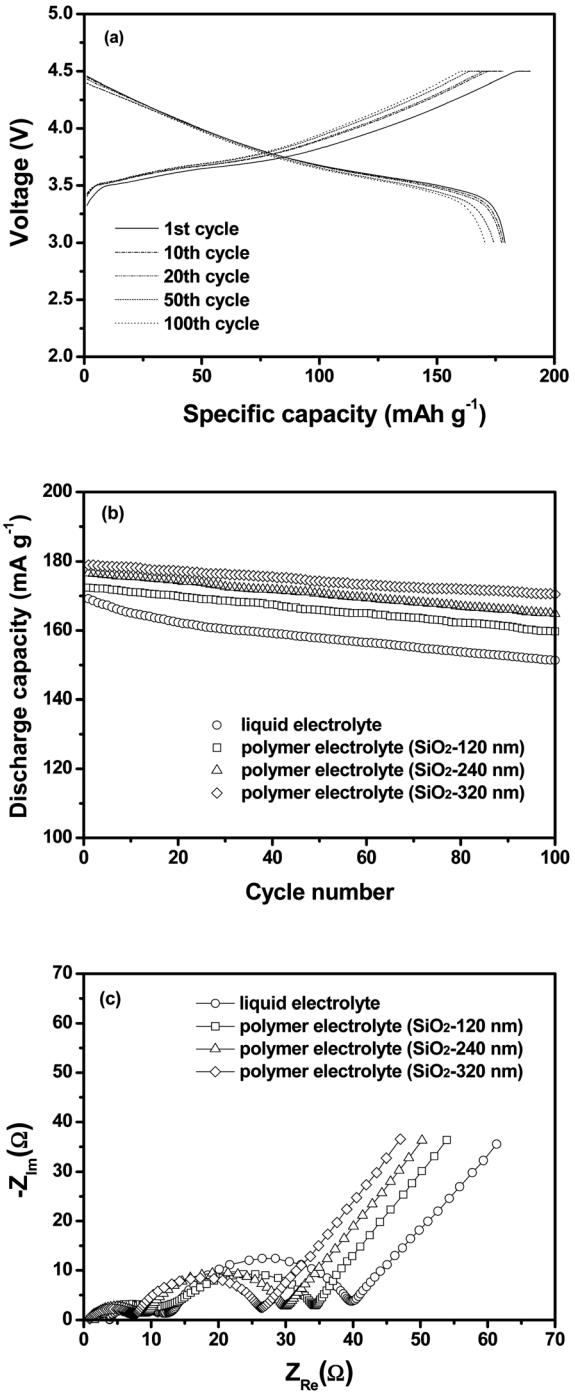

Fig. 7 (a) Charge and discharge curves of the lithium-ion polymer cell assembled with the composite polymer electrolyte containing $SiO_2(Li^+)$ particles with a shell thickness of 320 nm (0.5 C CC and CV charge; 0.5 C CC discharge; and cut-off, 3.0–4.5 V), (b) discharge capacities of the lithium-ion polymer cells assembled with the composite polymer electrolyte containing $SiO_2(Li^+)$ particles with different shell thicknesses, and (c) AC impedance spectra of lithium-ion polymer cells assembled with different composite polymer electrolytes, measured after 100 cycles.

exhibited higher initial discharge capacity and better capacity retention than did the cell with liquid electrolyte. The ionic conductivity of the liquid electrolyte used in this study is 7.1×10^{-3} S cm^{-1}. However, the ionic conductivity (1.3×10^{-4} S cm^{-1}) of the polypropylene separator filled with the electrolyte

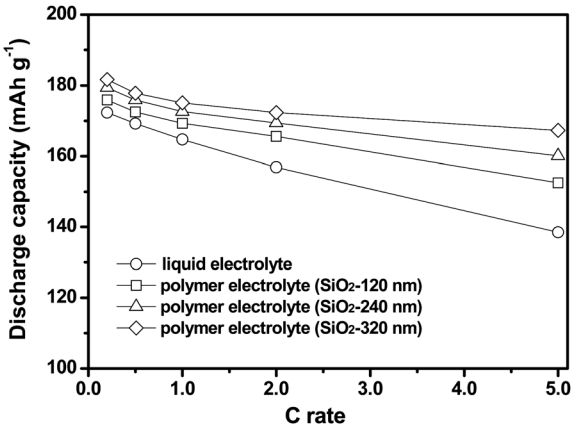

Fig. 8 Discharge capacities of lithium-ion polymer cells assembled with different composite polymer electrolytes, as a function of the C rate.

solution is much lower than that of the electrolyte solution, as the specific resistivity of the separator saturated with liquid electrolyte is increased by the combination of tortuosity and porosity of the separator. Thus, the ionic resistance is higher in the liquid electrolyte-based cells than in the cells assembled with composite polymer electrolytes, which gives rise to the reduction of initial discharge capacity. The hydrophilic PLLS in the shells of the $SiO_2(Li^+)$ particles holds the organic solvent more effectively, and the ability to retain the electrolyte solution in the composite polymer electrolyte is favored by the addition of $SiO_2(Li^+)$ powder. Fig. 7(c) compares the AC impedance spectra of the cells at the charged state after 100 cycles. The spectra exhibited two overlapping semicircles, which were assigned to the resistance of the electrode surface films (R_f) and the charge transfer resistance on the electrode–electrolyte interface (R_{ct}), respectively.[25,26] The electrolyte resistance (R_e) estimated from the intercept on the real axis in the high-frequency range decreased with increasing shell thickness of $SiO_2(Li^+)$. Total interfacial resistance (R_i) estimated from the summation of R_f and R_{ct} also decreased with increasing shell thickness of the $SiO_2(Li^+)$ particles. It is well known that the addition of inorganic fillers is effective for decreasing the electrode interfacial resistance.[27,28] The presence of larger amounts of hydrophilic PLSS in the shell of the $SiO_2(Li^+)$ particles was able to hold the solvent more effectively, which resulted in the enhancement of interfacial stability. The thick shell layer of $SiO_2(Li^+)$ particles was also able to assist in adhering the polymer electrolyte to the electrodes, which gave favorable interfacial charge transport between the electrodes and the electrolytes in the cell.

To evaluate the rate capability of the lithium-ion polymer cells, the cells were charged to 4.5 V at a constant current of 0.2 C and discharged at rates ranging from 0.2 C to 5.0 C. Fig. 8 shows that the shell thickness of $SiO_2(Li^+)$ affects the rate capability. The best performance was delivered by a cell assembled with $SiO_2(Li^+)$ with a 320 nm thick shell. As discussed earlier, both ionic conductivity and lithium transport number increase with increasing shell thickness, which reduces the concentration polarization in the cell during cycling and

provides high discharge capacity at high current rates. Also, favorable interfacial characteristics in the cell ensure cell operation at high current rates. Again, the response was much better than that of the cell with liquid electrolyte.

Conclusions

Core–shell structured SiO_2 nanoparticles with different core sizes and shell thicknesses were synthesized and used as fillers in Li^+-conducting composite polymer electrolytes. The composite polymer electrolytes containing core–shell $SiO_2(Li^+)$ nanoparticles with 320 μm thick shell layer exhibited high ionic conductivity, good mechanical strength and favorable interfacial characteristics. Lithium-ion polymer cells assembled with the composite polymer electrolytes were characterized by high capacity, good capacity retention and excellent rate performance. Our results suggest that the core–shell structured $SiO_2(Li^+)$ nanoparticles with controlled morphologies are promising fillers in the composite polymer electrolytes for lithium-ion polymer batteries with good capacity retention and high power capability.

Acknowledgements

This work was supported by the Energy Efficiency & Resources of the KETEP grant (20112010100110), the Human Resources Development of KETEP grant funded by the Korea Government Ministry of Knowledge Economy (no. 20104010100560) and the Basic Science Research Program through the National Research Foundation of Korea (NRF) grant funded from the Ministry of Education, Science and Technology (MEST) of Korea (no. 2012-0000591).

References

1 W. H. Meyer, *Adv. Mater.*, 1998, **10**, 439.
2 M. Armand, *Nature*, 2008, **451**, 652.
3 R. C. Agrawal and G. P. Pandey, *J. Phys. D: Appl. Phys.*, 2008, **41**, 223001.
4 V. D. Noto, S. Lavina, G. A. Giffin, E. Negro and B. Scrosati, *Electrochim. Acta*, 2011, **57**, 4.
5 E. Quartarone and P. Mustarelli, *Chem. Soc. Rev.*, 2011, **40**, 2525.
6 J. Y. Song, Y. Y. Wang and C. C. Wan, *J. Power Sources*, 1999, **77**, 183.
7 J. Hassoun, P. Reale and B. Scrosati, *J. Mater. Chem.*, 2007, **17**, 3668.
8 J. W. Fergus, *J. Power Sources*, 2010, **195**, 4554.
9 J. Fan and P. S. Fedkiw, *J. Electrochem. Soc.*, 1997, **144**, 399.
10 D. W. Kim and Y. K. Sun, *J. Electrochem. Soc.*, 1998, **145**, 1958.
11 F. Croce, G. B. Appetecchi, L. Persi and B. Scrosati, *Nature*, 1998, **394**, 456.
12 D. E. Strauss, D. Golodnitsky and E. Peled, *Electrochem. Solid-State Lett.*, 1999, **2**, 115.
13 N. Byrne, J. Efthimiadis, D. R. MacFarlane and M. Forsyth, *J. Mater. Chem.*, 2004, **14**, 127.
14 H. Han, W. Liu, J. Zhang and X.-Z. Zhao, *Adv. Funct. Mater.*, 2005, **15**, 1940.
15 A. S. Arico, P. Bruce, B. Scrosati, J.-M. Tarascon and W. Van Schalkwijk, *Nat. Mater.*, 2005, **4**, 366.
16 S. K. Das, S. S. Mandal and A. J. Bhattacharyya, *Energy Environ. Sci.*, 2011, **4**, 1391.
17 C. Tang, K. Hackenberg, Q. Fu, P. M. Ajayan and H. Ardebili, *Nano Lett.*, 2012, **12**, 1152.
18 N. S. Choi, Y. M. Lee, B. H. Lee, J. A. Lee and J. K. Park, *Solid State Ionics*, 2004, **167**, 293.
19 J. Sun, P. Bayley, D. R. MacFarlane and M. Forsyth, *Electrochim. Acta*, 2007, **52**, 7083.
20 J. Nordstrom, A. Matic, J. Sun, M. Forsyth and D. R. MacFarlane, *Soft Matter*, 2010, **6**, 2293.
21 Y. S. Lee, S. H. Ju, J. H. Kim, S. S. Hwang, J. M. Choi, Y. K. Sun, H. Kim, B. Scrosati and D. W. Kim, *Electrochem. Commun.*, 2012, **17**, 18.
22 Y. S. Lee, J. H. Lee, J. A. Choi, W. Y. Yoon and D. W. Kim, *Adv. Funct. Mater.*, 2012, DOI: 10.1002/adfm.201200692.
23 J. Evance, C. A. Vincent and P. G. Bruce, *Polymer*, 1987, **28**, 2324.
24 M. P. Seah and D. Briggs, *Practical Surface Analysis by Auger and X-ray Photoelectron Spectroscopy*, Wiley & Sons, 2nd edn, 1992.
25 A. Funabiki, M. Inaba and Z. Ogumi, *J. Power Sources*, 1997, **68**, 227.
26 M. D. Levi, G. Salitra, B. Markovsky, H. Teller, D. Aurbach, U. Heider and L. Heider, *J. Electrochem. Soc.*, 1999, **146**, 1279.
27 C. M. Yang, H. S. Kim, B. K. Na, K. S. Kum and B. W. Cho, *J. Power Sources*, 2006, **156**, 574.
28 S. J. Lim, Y. S. Kang and D. W. Kim, *Electrochim. Acta*, 2011, **56**, 2031.